

# Parametric Studies of Advanced Turboprops

J. G. Maser\* and D. G. Fertis†  
*University of Akron, Akron, Ohio*  
 and

R. A. Aiello‡ and C.C. Chamis§  
*NASA Lewis Research Center, Cleveland, Ohio*

The effects of geometric variables (sweep and twist) on the structural performance of advanced turboprops are investigated. The investigation is limited to aerodynamically efficient turboprops using an acceptable design configuration as a baseline. The baseline configuration is modified using a  $7 \times 7$  array of independently varying sweep and twist parameters while acceptable aerodynamic efficiency is maintained. The turboprop structural performance is evaluated in terms of critical speeds, tip displacements, and vibration frequencies where geometric nonlinearities are included. The results obtained are presented in such a manner as to highlight the effects of sweep and twist on the structural performance of aerodynamically efficient turboprop configurations.

## Introduction

THE potential for high propulsive efficiency in the Mach 0.7–0.8 range has, in recent years, renewed interest in propeller propulsion systems. Improved multibladed propellers, termed advanced turboprops, have the potential for reduced fuel consumption while maintaining the performance levels of modern turbofans. Advanced turboprop concepts feature thin, swept, and twisted propeller blades, often with complex structural properties. Such turboprop blades are twisted in order to obtain an efficient angle of attack at all points along the radius of the blade. Furthermore, the sweep angle produces a significant reduction in noise and is, therefore, a desirable design feature.

Traditionally, development of feasible advanced turboprop blades has involved a process of repeating trial configurations. Specifically, a swept and twisted turboprop blade would be developed based on advantageous aerodynamic characteristics, including the high efficiency and low noise previously mentioned, and then it would be considered for structural analysis. However, blades of this type (thin, highly swept, and twisted) exhibit a complex state of structural response under a centrifugal force field. Often, as a result, blades that were aerodynamically desirable were not structurally feasible. This conflict necessitated the development of new blade configurations, with the structural limitations of the previous designs kept in mind. However, relatively few blade configurations (fewer than eight) have been developed and investigated, and it is not known exactly how the structural limitations of each configuration may be related.

The objective of this paper is to describe a study conducted to investigate the effects of sweep and twist on the structural response of aerodynamically efficient (within a range) turboprop configurations under a centrifugal force field.<sup>1</sup> Specifically, an existing, representative advanced turboprop,

named SR5, was used as a model on which variations of sweep and twist were made. An available aerodynamic propeller performance analysis program computer code was used to establish an array of aerodynamically efficient turboprop blade configurations. The array contains blades with 7 different sweeps and 7 different twists for a total of 49 combinations. This paper includes summaries of analyses and significant results. Extensive discussions and details are provided in Ref. 1.

## Turboprop Geometry and Analysis

A representative turboprop stage and propeller blade (turboprop) with the Cartesian coordinate axes are shown in Fig. 1. The sweep angle of a turboprop is defined as the angle measured from the plane of rotation to the 50% chord line (midchord). Therefore, the larger the sweep angle, the more swept the blade is. This definition may be used to specify the sweep at any radius  $r$ , where radius corresponds to the  $x$  axis and is defined as the distance from the center of rotation on the line formed by the intersection of the plane of rotation and the plane of forward velocity of the propeller. The characteristic sweep value assigned to a given turboprop blade is defined as the sweep at  $3/4$  of the radius from the center of rotation to the tip of the blade,  $3/4 R$ . The blade sweep definition is shown in Fig. 2.

The twist angle of a propeller blade is defined as the angle measured from the plane of rotation to the chord line in a

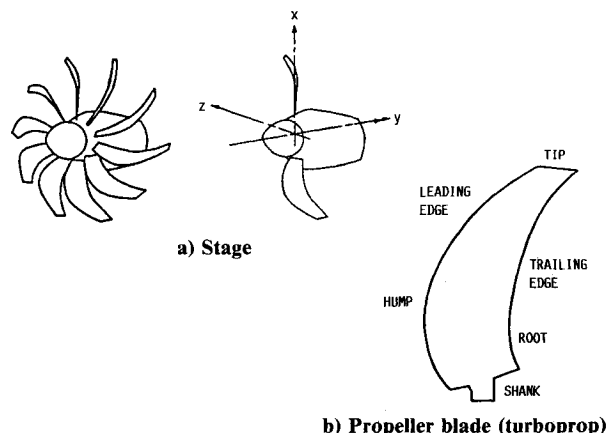


Fig. 1 Representative turboprop stage and propeller (turboprop).

Received March 8, 1988; presented as Paper 88-2266 at the AIAA/ASME/ASCE/AHS/ASC 29th Structures, Structural Dynamics and Materials Conference, Williamsburg, VA, April 18-20, 1988; revision received Sept. 28, 1988. Copyright © 1988 American Institute of Aeronautics and Astronautics, Inc. No copyright is asserted in the United States under Title 17, U.S. Code. The U.S. Government has a royalty-free license to exercise all rights under the copyright claimed herein for Governmental purposes. All other rights are reserved by the copyright owner.

\*Former graduate student.

†Professor, Civil Engineering.

‡Senior Aerospace Engineer, Structures Division.

§Senior Aerospace Scientist, Structures Division.

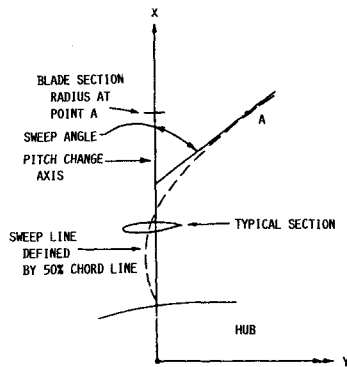


Fig. 2a Blade sweep definition.

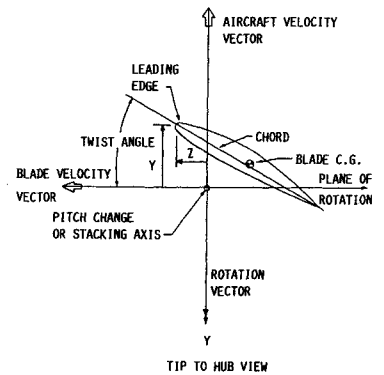


Fig. 3 Blade twist definition.

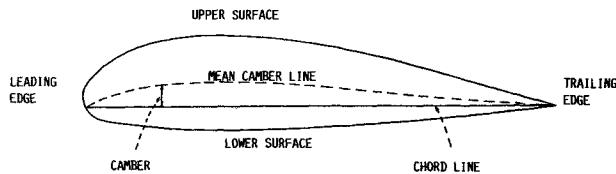


Fig. 2b Typical airfoil section.

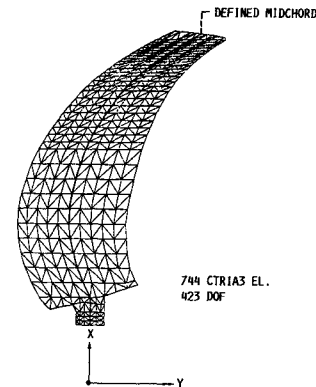


Fig. 4 Turboprop finite-element model.

plane normal to the pitch change axis, where the axis corresponds to the radius line and  $x$  axis (Fig. 3). For propellers, the twist angle is large near the hub and decreases toward the tip. Therefore, it is important to realize that a decreasing twist angle means an increase in the actual structural twist of the blade. As with sweep, the twist angle definition may be used to specify twist at any radius  $r$ , but the characteristic twist angle assigned to a given turboprop blade is defined as the twist at  $3/4 R$ .

#### Representative SR5 Turboprop Description and Analysis Model

The finite-element model representative SR5 turboprop blade used as the baseline for the parametric studies is shown in Fig. 4. The blade is solid titanium and is approximately 10 in. long with a tip chord of 2 in. and a maximum chord at the hump of 3.8 in. Thickness varies from 1 in. at midchord at the root to 0.04 in. at midchord at the tip. The leading-edge thickness varies from 0.180 in. at the root to 0.022 in. at the tip. The trailing-edge thickness varies from 0.77 in. at the root to 0.016 in. at the tip. The SR5 has a twist angle of 66.0 deg and a sweep angle of 30.7 deg (tip sweep of 63 deg). The total weight of the SR5 is 0.719 lb.

The coordinate system for SR5 and subsequent turboprop configuration variations is Cartesian and defined as shown in Figs. 1 and 4. The  $x$  origin is at the center of the hub, and the  $y$  origin is at the midchord of the shank.

The finite-element analysis model (Fig. 4) consists of 423 grid points and 744 CTIA3 elements.<sup>2-4</sup> For convenience, the midchord is defined to be the sixth node in from either the leading or trailing edge on any given chord line. All chords are defined in the  $y$ - $z$  plane. The sweep at any radius was based on the tangent to the line connecting the midchords. The midchord definition is not exactly the 50% chord line; however, it is very close and used consistently in all the turboprop configurations of the parametric studies. This finite-element model was used to evaluate the structural performance of the propeller (displacements, frequencies, critical speeds), including the effects of geometric nonlinearity.

A graphical approach was employed to vary sweep in a relatively uniform manner. Specifically, the SR5 midchord line was plotted from existing data; and six new midchord lines were constructed in order to retain the characteristics of the SR5 while successively decreasing the sweep. Sweep in-

creases were not considered because previous investigation indicated that the SR5's high degree of sweep resulted in significant excursions in tip displacements at relatively low angular speeds.<sup>5</sup> Such differences are considered indicative of the onset of structural instability and, as a result, the SR5 was regarded as the high end limit to sweep.

#### Turboprop Aerodynamic Performance

A computer code based on strip analysis was used to evaluate the performance of the turboprops (propellers) for a given set of conditions. The output of this code includes values such as drag-to-lift ratios, sectional efficiencies, sectional losses, and sectional Mach numbers, all given at Gauss stations. In addition, the thrust and apparent efficiency at the propeller are provided.

The apparent efficiency is based on the apparent thrust of a propeller operating in a region of reduced velocity due to the presence of a body behind it. In brief, efficiency ( $\eta$ ) is defined as

$$\eta = \frac{\text{power output}}{\text{power input}} = \frac{TV}{2\pi nQ}$$

where  $T$  = thrust,  $V$  = forward speed of airplane,  $n$  = rotational speed, and  $Q$  = torque.

The elemental thrust is the force produced by the blade element along the line of flight and is determined from elemental lift forces minus elemental drag forces taken along this line. The elemental torque is the force produced by the blade element resisting rotation multiplied by the radial distance to the center of rotation and is determined from the elemental lift plus elemental drag taken along the plane of rotation.

Because aerodynamic performance was evaluated only as a simplified means of establishing reasonable limits on specific propeller configurations, detailed theory is beyond the scope of this paper. However, more detailed theory may be found in Refs. 6-8. The array summarizing the parametric studies performed is described in Tables 1 and 2. The input data are summarized in Table 3.

## Results and Discussion

### Aerodynamic Performance

The aerodynamic performance of each turboprop blade was evaluated primarily as a simplified means of establishing reasonable limits to the range of sweep and twist to be investigated. Therefore, the criterion judged to be the best overall representation of aerodynamic performance of a given propeller blade was apparent efficiency. The basis used for establishing limits on apparent efficiency is the data from a high-speed propeller performance study shown in Fig. 5 (Ref. 9). As can be seen, at any Mach number, design efficiencies vary by a relatively small amount (on the order of 3%). As a result, it was established that relatively large drops in apparent efficiency (3-4%) from any encountered maximum would make a con-

figuration aerodynamically unacceptable. Therefore, based on this criterion, the 49 turboprop configurations previously observed and defined in Table 2 were established. (Details of the results are forthcoming.)

In addition to establishing limits to the configuration matrix, this analysis provided some meaningful information concerning the effects of sweep and twist variation on the apparent efficiencies of a propeller. It is noted that investigation of design speed variations for each specific configuration was beyond the scope of this study and, as a result, all of the configurations were evaluated aerodynamically at the same rotational speed.

The effects of sweep variations on apparent efficiencies are shown in Fig. 6 for lines of constant twist. Figure 7 shows the effects of twist variations on apparent efficiencies for lines of constant sweep. Note that only the turboprop 49 configurations considered aerodynamically reasonable are shown and that the approximate lower efficiency limit is evident. The blade configurations considered unreasonable were exhibiting apparent efficiencies of approximately 75%.

From Figs. 6 and 7, it is generally observed that the apparent efficiencies are more sensitive to twist variations. Spec-

**Table 1 Range of sweep and twist variations: sweep increases proportionately with angle; twist increases inversely with angle<sup>a</sup>**

Sweep		Twist	
Label	Angle, deg	Label	Angle, deg
A	14	A	73
B	16	B	71
C	20	C	69
D	23	D	68
E	26	E	66
F	29	F	64
G	31	G	62

<sup>a</sup>Letters refer to cases studied in combination, as shown in Table 2.

**Table 2 Blade configuration matrix showing 49 combinations: sweep increases from left to right; twist increases from top to bottom<sup>a</sup>**

AA	BA	CA	DA	EA	FA	GA
AB	BB	CB	DB	EB	FB	GB
AC	BC	CC	DC	EC	FC	GC
AD	BD	CD	DD	ED	FD	GD
AE	BE	CE	DE	EE	FE	GE
AF	BF	CF	DF	EF	FF	GF
AG	BG	CG	DG	EG	FG	GG

<sup>a</sup>The respective angles are shown in Table 1. For example, AC is 14 deg sweep with 69 deg twist.

**Table 3 Aerodynamic propeller characteristics**

Aerodynamic characteristics independent of blade radial distance										
Number of blades	= 10									
Blade diameter	= 24.1 in.									
Spinner cutoff point	= 0.212 $r/R$									
Shaft horsepower	= 104.8									
Propeller rotational speed	= 5709 rpm									
Altitude	= 35000 ft									
True airspeed	= 461.2 knots, = Mach 0.79									
Type of airfoil	= NACA Series 16 compressible									
Aerodynamic characteristics dependent on radial distant (values correspond to Gauss stations)										
Gauss station	0.9902	0.9489	0.8787	0.7856	0.6779	0.5652	0.4575	0.3644	0.2942	0.2529
Thickness/chord	0.018	0.018	0.021	0.024	0.031	0.039	0.051	0.068	0.104	0.175
Chord/diameter	0.1079	0.1248	0.1326	0.1454	0.1562	0.1602	0.1550	0.1506	0.1466	0.1452
Design lift coeff.	0.207	0.221	0.234	0.235	0.213	0.180	0.100	0.060	0.020	0.005
Velocity ratio	1.036	1.025	1.005	0.983	0.960	0.940	0.894	0.850	0.815	0.800
7 twist configurations at the Gauss stations										
Twist A	- 6.57	- 5.31	- 2.83	- 0.73	1.53	4.05	6.96	8.57	9.08	9.64
Twist B	- 7.49	- 6.05	- 3.21	- 0.82	1.76	4.68	8.12	9.95	10.63	11.24
Twist C	- 8.29	- 6.73	- 3.62	- 0.90	1.98	5.39	9.30	11.40	12.19	12.92
Twist D	- 9.18	- 7.48	- 4.09	- 1.02	2.19	5.97	10.44	12.82	13.71	14.56
Twist E	- 9.39	- 8.14	- 4.42	- 1.14	2.44	6.66	11.64	14.40	15.35	16.25
Twist F	- 10.68	- 8.75	- 4.84	- 1.24	2.66	7.31	12.88	15.91	17.03	18.04
Twist G	- 11.32	- 9.29	- 5.13	- 1.33	2.91	8.01	14.16	17.56	18.73	19.91
7 sweep configurations at the Gauss stations										
Sweep A	29.73	24.80	18.21	13.71	8.42	4.12	2.18	- 16.96	- 21.31	- 29.77
Sweep B	31.30	28.90	25.97	18.11	11.26	7.13	2.75	- 16.96	- 21.31	- 29.77
Sweep C	37.09	36.10	27.43	22.49	13.71	9.37	3.26	- 16.96	- 21.31	- 29.77
Sweep D	42.55	41.67	36.61	27.34	15.38	11.42	3.72	- 16.96	- 21.31	- 29.77
Sweep E	46.94	46.10	41.89	31.13	18.52	11.70	3.55	- 16.96	- 21.31	- 29.77
Sweep F	53.91	51.83	44.97	33.43	20.20	12.84	3.38	- 16.96	- 21.31	- 29.77
Sweep G	62.44	58.39	48.49	34.22	23.37	13.93	- 0.46	- 16.96	- 21.31	- 29.77

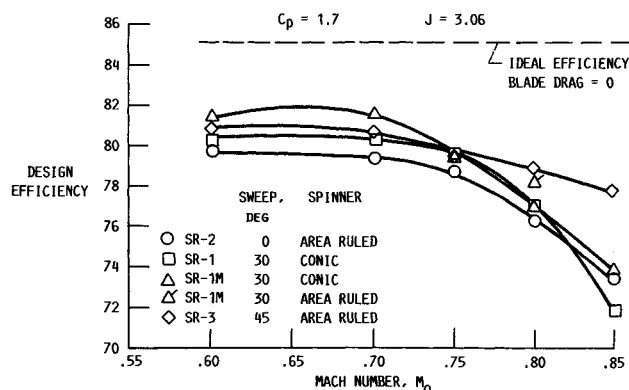


Fig. 5 High-speed propeller performance summary based on strip analysis.

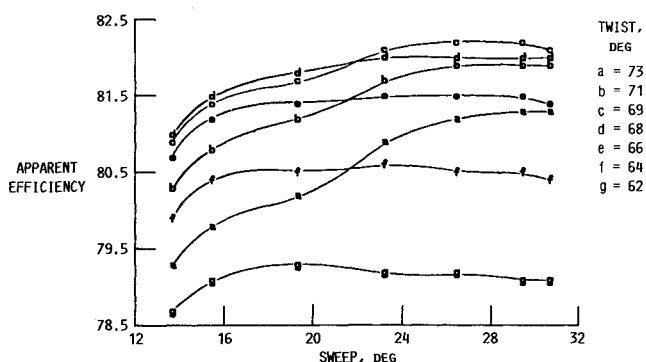


Fig. 6 Effect of sweep on apparent efficiency for lines of constant twist.

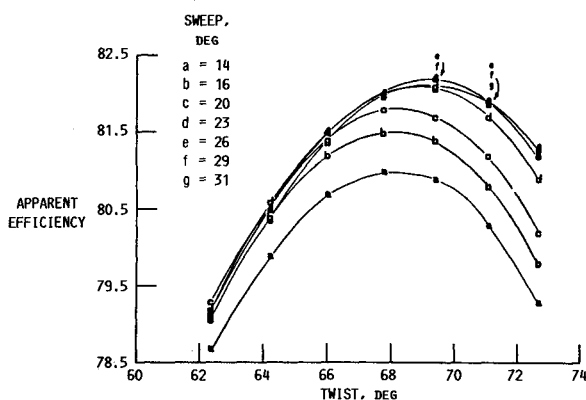


Fig. 7 Effect of twist on apparent efficiency for lines of constant sweep.

fically, for lines of constant sweep, the efficiencies pass through a pronounced maximum as twist increases. The maximum generally occurs in a twist region of 67 to 70 deg. On the other hand, for lines of constant twist, the efficiencies are not as consistent with increasing sweep. In particular, for the higher twisted configurations, efficiencies increase and then level off with increasing sweep. For the lower twisted configurations, efficiencies increase steadily with increasing sweep and just begin to level off at the highest sweep considered. Therefore, increases in sweep affect efficiencies more for lower twisted configurations than for higher twisted configurations. As an aside, it can be pointed out that, for the aerodynamic analysis, the sweep and twist angles are defined at Gauss stations. Thus, the manner in which sweep and twist are varied along the radius of the blade have significant effects on

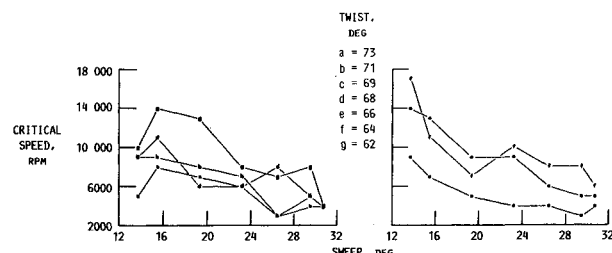


Fig. 8 Effect of sweep on critical speed for lines of constant twist.

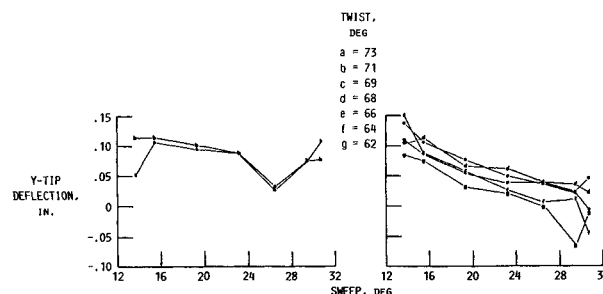


Fig. 9 Effect of sweep on y-tip deflection for lines of constant twist.

the results, even if the defined sweep and twist values remain the same.

#### Critical Speeds

The critical speed referred to, presently and in future context, is the rotational speed (rpm) at which the geometric nonlinear solution no longer converges for that particular blade configuration. At this point, tensile buckling<sup>10</sup> would occur. Each configuration was evaluated in load increments of 1000 rpm until the critical speed was found. Generally, the number of iterations required for convergence range from 3 to 18.

Figure 8 shows critical speeds as a function of sweep for lines of constant twist. These results are not intuitively obvious because the curves do not exhibit relatively smooth transitions. The curves reflect, in part, the complex interaction effects of propeller geometry that may be observed in experimental data. These curves indicate the following general trends: 1) the critical speed decreases as sweep increases, and 2) the critical speed increases as twist increases. (Recall that, as twist angle decreases, the actual twist increases.) The highest values for critical speed occurred at low sweeps and high twists, whereas the lowest values occurred at high sweeps and low twists.

#### Tip Displacements

Tip displacements are defined with respect to the midchord of the blade tip and are taken at the last rpm at which the nonlinear solution converged (critical speed, 1000 rpm). Three types of displacements are considered (Fig. 1): y-tip deflection, z-tip deflection, and tip-chord rotation. The y-tip deflection is defined as the deflection in the plane of the forward velocity of the propeller (x-y plane by current coordinate system). The effects of sweep on y-tip deflections for constant twist angles are shown in Fig. 9. The effects of sweep on z-tip deflections for constant twist angles are shown in Fig. 10. Tip-chord rotation is defined as the change in the blade tip-chord twist angle in a plane normal to the pitch change axis (y-z plane by current coordinate system). The effects of sweep on tip-chord twist angle for constant twist angle are shown in Fig. 11.

The significant observations from the results in Figs. 9-11 is that the structural behavior of swept, twisted turboprops is

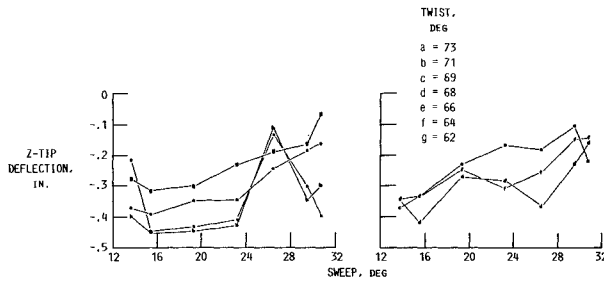


Fig. 10 Effect of sweep on z-tip deflection for lines of constant twist.

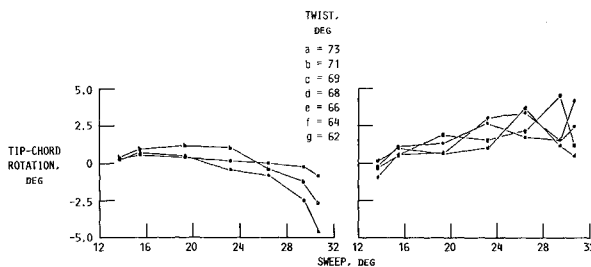


Fig. 11 Effect of sweep on tip-chord rotation for lines of constant twist.

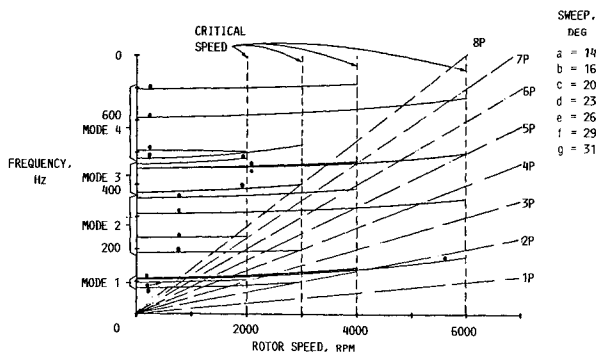


Fig. 12 Campbell diagram with rotor excitations for variable sweep, constant twist A (73 deg).

very complex and requires equally complex structural analyses to be evaluated. A consequence of this observation is that scaling of experimental data generally requires considerable judgment and care.

#### Vibration Frequencies

The vibration frequencies in the design speed range are important in stability and life assessment of the blade. In design practice, these are generally evaluated using the interference of vibration frequencies with rotor excitation orders, such as one per revolution (1P), two per revolution (2P), etc., are important in actual design practice. Figure 12 illustrates the effects of varying sweep with constant twist A (73 deg) on a frequency rotor speed (Campbell) diagram, where the critical speeds are also shown. The frequencies increase as the critical speed is approached; however, these increases are very slight. Furthermore, for each mode, as sweep increases, the frequencies generally decrease, the exception being sweep E (26 deg) in the third mode, which has the highest frequency for that mode.

#### Summary

The summary of results and conclusions of a parametric study to investigate the structural performance of advanced turboprops is as follows:

1) Critical speeds for constant twists decrease as sweep increases and, for constant sweeps, increase as twist increases. The highest values of critical speed occur for low-sweep, high-twist configurations, whereas lowest values occur for high-sweep, low-twist configurations.

2) The y-tip deflections only indicate a straightening of sweep for high-sweep, high-twist blade configurations.

3) The z-tip deflections for constant twists decrease as sweep increases and, for constant sweeps, decrease as twist increases. The largest z-tip deflections occur for high-sweep, high-twist configurations.

4) The tip-chord rotations indicate that turboprop blades with low twist pass from being more twisted to highly untwisted as sweep increases, whereas blades with high twist become more twisted as sweep increases. Tip-chord rotations for blades with low sweep become slightly more twisted as twist increases whereas blades with high sweep have rotations that pass distinctly from being untwisted to being more twisted as twist increases.

5) Large sweep variations have more diverse overall effects on critical speeds and displacements than do large twist variations.

6) Critical speeds are lower in configurations where tip-chord rotations are significant (either more twist or untwist) and higher when rotations are small.

7) For blade configurations with high sweep and high twist, displacements are dominated by tip-chord rotations. For blade configurations with low sweep and low twist, displacements are dominated by z-tip deflections.

8) Vibration frequencies at 0 rpm and constant twist decrease with increasing sweep for the first four modes. Similarly, vibration frequencies for low-sweep configurations at 0 rpm decrease with increasing twist, but only for the first and second modes. For the third and fourth modes, vibration frequencies increase with increasing twist for low-sweep configurations. For high-sweep configurations, frequencies increase with increasing twist for the first four modes.

#### References

- Maser, J. G., "A Parametric Study of Highly Swept Advanced Turboprops," NASA CR, in preparation.
- McCormick, C. W. (ed.), "MSC/NASTRAN User's Manual," MacNeal-Schwendler Corp., Los Angeles, CA, April 1982.
- Joseph, J.A. (ed.), "MSC/NASTRAN Application Manual," MacNeal-Schwendler Corp., Los Angeles, CA, 1981.
- MacNeil, R. H., "The NASTRAN Theoretical Manual," NASA SP-221(01), 1972.
- Aiello, R. A. and Chamis, C. C., "Large Displacement and Stability Analysis of Nonlinear Structures," NASA TM-82850, 1982.
- Goldstein, S., "On the Vortex Theory of Screw Propellers," *Proceedings of the Royal Society of London*, Vol. A123, 1929, pp. 440-465.
- Theodorsen, T., *Theory of Propellers*, McGraw-Hill, New York, 1948.
- Dommasch, D. O., Sherby, S. S., and Connolly, T. F., *Airplane Aerodynamics*, 5th ed., Pitman, New York, 1967.
- Mitchell, G. A., "Lifting Line Strip Analysis Propeller Performance Summary," unpublished research data, NASA Lewis Research Center, Cleveland, OH, 1981.
- Chamis, C. C. and Aiello, R. A., "Tensile Buckling of Advanced Turboprops," NASA TM-82896, 1982.